Wall Plume Induced by a Line Fire

by S. Chowdhury, G. Lleonart, V. Beck

Victoria University of Technology
Department of Mechanical Engineering
P O Box 14428, MMC, Melbourne 3000
Victoria, Australia

Abstract:

In this paper, a physical model of a wall plume adjacent to an adiabatic wall is presented. An analysis based on scaling and similarity assumptions has been carried out for the primary flow variables in the plume. The results obtained from the model and the analysis match well. An analytical expression for the velocity distribution in the plume is presented and it has been found to correlate with experimental results satisfactorily.

1. Introduction:

Fire accidents are one of the major hazards to human life and property. In a fire scenario, its developments can be divided into two stages; pre-flashover and post-flashover. Usually flashover is defined as the transition from a developing to a fully developed fire in which all the combustible items in the region have been engulfed by the fire. In the pre-flashover stage all the fires go through the important initial coherent phase where buoyant gases rise above the area of the fire source which is undergoing combustion, thus entraining the surrounding uncontaminated air. This buoyant flow, including any flames at the beginning is known as a fire plume. In a room with a fire source on the floor the plume rises and hits the ceiling where it bends and keeps propagating as a ceiling jet. Plume generated by a line fire on the floor and close to a wall is termed as a wall plume and needs to be investigated in detail to characterise the complete flow domain including the ceiling jet.

Theoretical analyses of plumes can be divided into two types; (1) integral methods based on averaging across the plume layer and (2) finite difference or differential methods which attempt to solve the full partial differential equations of transport in the space considered. In this paper, the discussion and analyse will be confined to the former method. There have been numerous publications concerning free plumes. For example the classic works of Morton et. al. (1956), Rouse et. al. (1952), Lee and Emmons (1961). A comprehensive review of plumes and ceiling jets can be found from List (1982) and Beyler (1986). Although wall plumes are similar to free plumes few studies have been done in this area. Nonetheless, numerous publications which describe laminar and turbulent flow development close to an adiabatic or isothermal wall may be found, see Gebhart (1988). Grella and Faeth (1975), studied a two dimensional thermal plume adjacent to an adiabatic vertical wall experimentally and measured the mean velocity and weight density defect profiles in the plume. Sparrow et. al. (1978) carried out a numerical study on wall and free plumes for a range of Prandtl Numbers.

The present study deals with a flow induced by a line fire on the floor and adjacent to a vertical wall with side walls on both sides. The end effects due to the side walls are considered to be negligible. Thus the flow can be considered as two dimensional and analysed in cartesian coordinates. In the following sections an analytical model and a similarity analysis have been put forward to characterise this type of flow. Also a conjecture is presented for the velocity distribution in the plume.

2. Theory:

The current analysis is based on a method similar to that employed by Alpert (1975) in the study of a turbulent ceiling jet. In deriving the conservation equations governing the plum flow, the following simplifying assumptions have been made.

i) The Boussinesq Approximation $\frac{\Delta\rho}{\rho_\infty} >> 1$ is valid.

ii) The flow is fully turbulent and steady in any time scale which is considered large compared to the scale in turbulence fluctuations.

iii) The velocities are much less than sonic velocity.

iv) The motion is two dimensional.

Conservation Equations:

Referring to the control volume in the flow domain, see Figure 1, and making the above assumptions the following conservation equations can be derived.

Equation of state: $\rho T = \rho_\infty T_\infty = \text{constant}$. ...(1)

Equation of mass conservation:

$$\frac{d}{dx}\int_0^\infty u_x \, dy = VE \qquad ....(2).$$

where, E is the entrainment coefficient and V is defined by the equation (5).

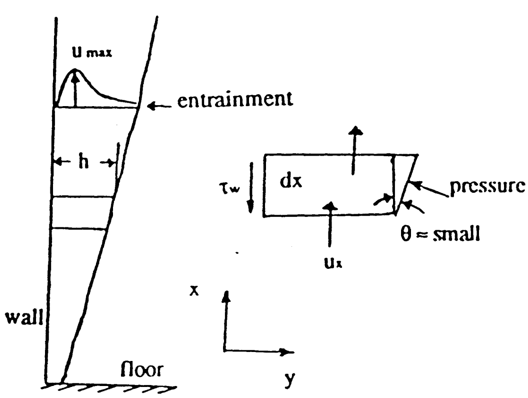

Fig 1: Schematic Diagram of the Flow

Equation of conservation of momentum,

$$\frac{d}{dx}\int_0^\infty u_x^2 dy = \int_0^\infty \frac{g(\rho-\rho_\infty)}{\rho_\infty} dy - \frac{\tau_w}{\rho_\infty} \qquad ....(3)$$

where τ_w = shear stress at the wall.

Equation of conservation of energy,

$$q'' = -\frac{d}{dx}\int_0^\infty \rho u_x c_p (T - T_\infty) \, dy \qquad ...(4)$$

Averaging the conservation equation:

The governing equations can be transformed into simpler form by employing average quantities over the thickness of the wall plume layer by a technique which is similar to the method used by Alpert (1975). These spatial averages are,

$$\int_0^\infty u_x \, dy = Vh \qquad ....(5)$$

$$\int_0^\infty u_x^2 \, dy = V^2 h \qquad ....(6)$$

$$\int_0^\infty \frac{g(\rho-\rho_\infty)}{\rho_\infty} dy = Dh \qquad ....(7)$$

$$\int_0^\infty \frac{u_x(\rho-\rho_\infty)g}{\rho_\infty} = VDh \qquad ....(8)$$

Thus, after the transformations the conservation equations become,

$$\frac{d}{dx}(Vh) = VE \qquad ....(9)$$

$$\frac{d}{dx}(V^2 h) = Dh - C_f V^2, \qquad C_f = \frac{\tau_w}{\rho_\infty V^2} \qquad ...(10)$$

$$Q'' = -\frac{q''g}{c_p T_\infty \rho_\infty} = \frac{d}{dx}(VDh) \qquad ....(11)$$

A further transformation is applied to these equations with respect to the initial conditions of the plume, at x = 0, V = Vo, D = Do, and h = ho. The variables introduced are,

$\chi=\frac{x}{ho}$, $V^*=\frac{V}{Vo}$, $D^*=\frac{D}{Do}$, and $\eta=\frac{h}{ho}$. Thus after the transformations the conservations equations are,

$$\frac{d}{d\chi}(V^*\eta) = V^*E \qquad \text{.............(12)}$$

$$\frac{d}{d\chi}(V^{*2}\eta) = \frac{D^*\eta}{Fro^2} - CfV^{*2} \qquad \text{.........(13)}$$

$$\ddot{Q} = \frac{d}{d\chi}(V^*D^*\eta) \qquad \text{.............(14)}$$

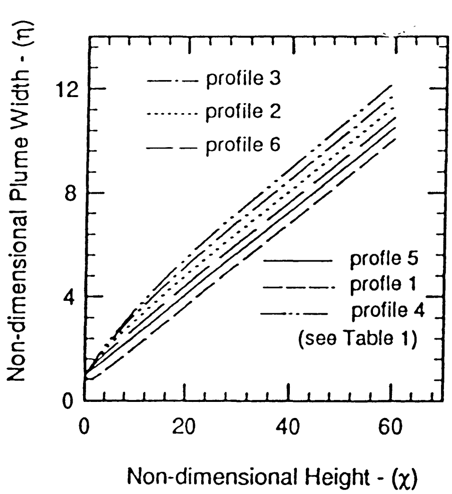

Fig. 2. Streamwise plume width variation

where, Fro= the initial Froud Number = $\frac{Vo}{\sqrt{Doho}}$, and $\ddot{Q} = -\frac{q''g}{c_pT_\infty\rho_\infty VoDo}$. .....(15)

The equations (12) - (14) are coupled and these have been uncoupled to arrive at simpler relations, which are as follows,

$$\frac{dV^*}{d\chi} = \frac{D^*}{V^*}\frac{1}{Fro^2} - \frac{V^*}{\eta}(Cf + E) \qquad \text{........(16)}$$

$$\frac{d\eta}{d\chi} = (2E + Cf) - \frac{D^*\eta}{V^{*2}}\frac{1}{Fro^2} \qquad \text{.......(17)}$$

$$\frac{dD^*}{d\chi} = \frac{\ddot{Q} - EV^*D^*}{V^*\eta} \qquad \text{.................(18)}$$

with the initial conditions at $\chi = 0$, $V^*_o = D^*_o = \eta_o = 1$ ....(19).

3. Numerical Analysis:

Equations (16) to (18) were solved numerically using a differential equation solver. Solutions are presented five different initial conditions which are shown in Table 1. Note that the initial density defect of 6.2 $(\frac{m}{s^2})$ corresponds to an initial temperature difference of 796 K which is considered to be the origin of a thermal plume, see Hasemi et. al., 1986. The results of these conditions in non-dimensional parameters are presented in Fig 2 to 6. The coefficient of entrainment, E, is taken as 0.16 which was the value used by Lee and Emmons (1961). In a later section the consequences of using different entrainment coefficient is examined. The friction factor Cf is taken as 0.001 and it has been found that using friction factors, ranging from 0.01 to 0.001, does not alter the results appreciably The changes in V and Fr are only of the order of 2% whereas for D and h it is much less. Hence in subsequent analysis it has been taken as 0.001. Fig 2 shows the variation of the plume width with height. Apart from close to the plume origin, the growth is linear with height.

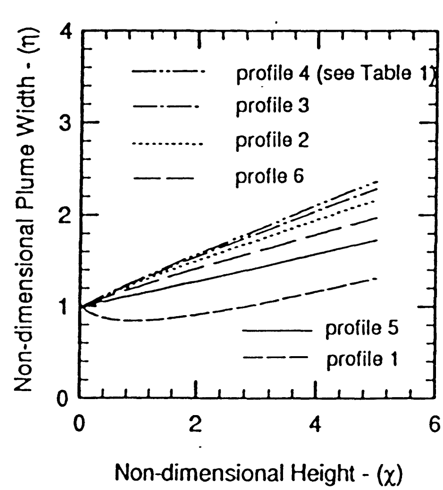

Fig. 3. Plume width near the origin

Table 1 : Initial Conditions for the Wall Plume

Profile no.	Vo	Do	ho	Fro
1	.592	6.2	.05	1.0632
2	2.369	6.2	.05	4.2548
3	2.962	6.2	.05	5.3199
4	3.554	6.2	.05	6.3831
5	1.25	6.2	.05	2.245
6	1.77	6.2	.05	3.179

Close to the origin the variation of the width is shown in Fig 3. In profile no. 1, where the initial velocity is low, a necking formation may be observed which shows due to high buoyancy force the fluid accelerates and entrains more and more ambient fluid. After a certain height, it behaves as other plumes and spreads linearly. Fig 4 shows the streamwise velocity variation. It may be observed that after a certain height the velocity remains constant. Fig 5 represents the density defect or temperature variation in the flow and it appears to vary inversely with

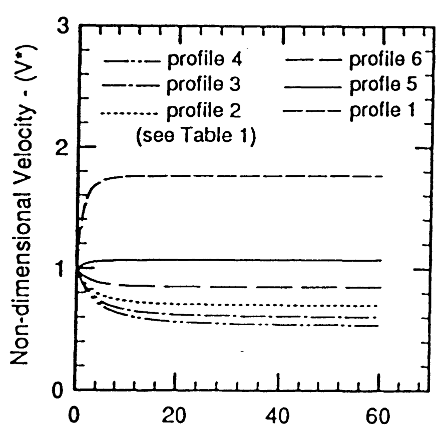

Fig. 4. Streamwise velocity variation

height. The change in Froud number, shown in, in Fig 6, approach a constant value in all cases. Thus the suggestions drawn from these observations are,

$$\left.\begin{array}{l} V \sim \text{const.} \\ D \text{ or } T_{avg} \sim \dfrac{1}{x} \\ h \sim x \\ Fr \sim \text{const.} \end{array}\right\} \qquad \text{.............(20)}$$

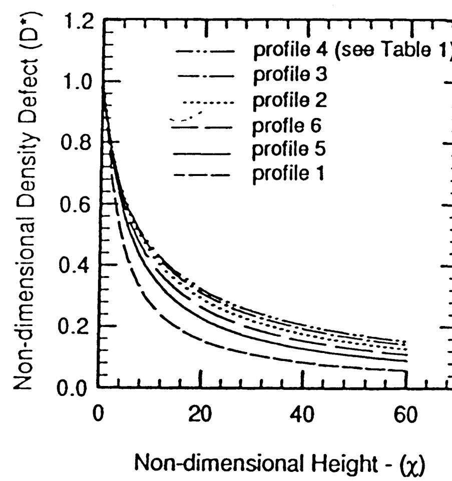

Fig. 5. Streamwise density defect variation

<u>Entrainment Coefficient:</u>

In general, entrainment is considered to depend on buoyancy and position. In this model it was assumed that entrainment occurs at the outer edge of the plume where the streamline velocity was negligible. In the past, researchers have taken this entrainment to be a linear function of the average or maximum streamwise velocity in the profile. This is represented in the following expression,

$$u_{ent.} = EV \qquad \text{............(21)}$$

where, E is the coefficient of entrainment and taken as constant. Various values of E have been taken in the past, for example 1) 0.082 by Morton (1959), 2) 0.125 by Morton et. al. (1956), 3) 0.16 by Lee and Emmons (1961). The effect of choosing these values have been examined in Fig. 7 to Fig. 11. Instead of taking

E as constant, it can also be presented as a function of buoyancy. Similar approach was considered by Alpert (1975) for entrainment in a ceiling jet. The entrainment is governed by the expression,

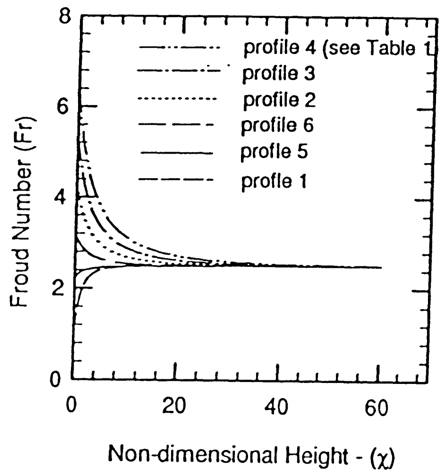

Fig. 6. Streamwise Froud number variation

$$E = E_j \exp\left(-\frac{\alpha}{Fr^2}\right) \quad ....(22)$$

where Ej can be determined from the initial conditions and $\alpha = 3.9$ (Alpert, 1975). E at origin is taken as 0.12. Graphs are plotted in Fig. 7 to Fig. 11 using equation (22). It is interesting to note that because the Froud. No. tend to approach same quantity, entrainment coefficient would be virtually constant after a certain distance.

4. Scaling Analysis and Velocity Distribution in Wall Plumes:

The following length, velocity, and temperature scales are defined for the wall plume.

L: streamwise length scale,
h: cross-stream length scale

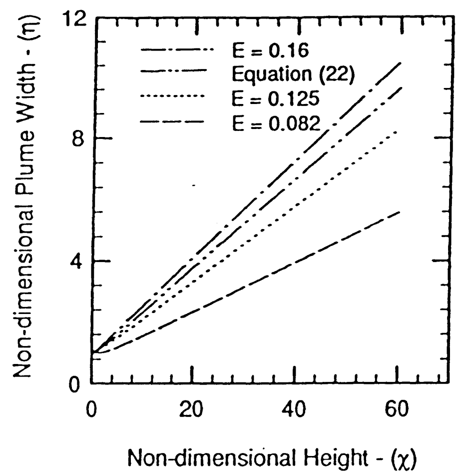

Fig. 7. Plume width variation with entrainment

u_m, v : velocity scales,
$\tilde{u}$, $\tilde{v}$: velocity fluctuations,
T: temperature scale,
$\tilde{\theta}$: temperature fluctuation

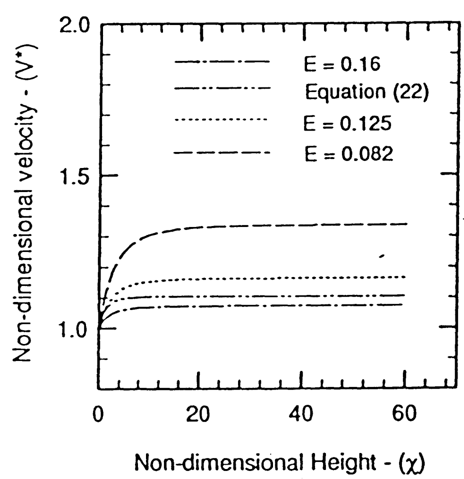

Fig. 8. Velocity variation with entrainment

Using these scales, an order of magnitude analysis is carried out, see Tennekes and Lumley

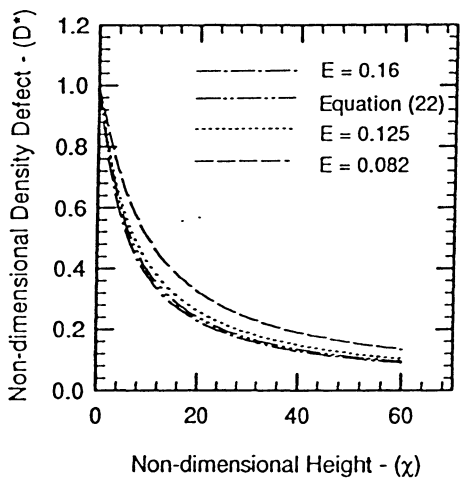

Fig. 9. Density defect variation with entrainment

(1972), on the momentum and energy transport equations which are shown below. The assumption is made that the flow is self similar and parallel in this situation.

Momentum:

$$u\frac{\partial u}{\partial x}+v\frac{\partial u}{\partial y}+\frac{\partial}{\partial y}(\overline{uv})=\frac{g(T-T_a)}{T_a} \quad ...(23)$$

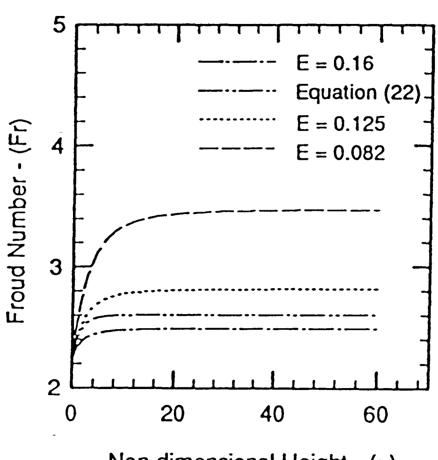

Fig. 10. Froud number variation with entrainment

Energy:

$$u\frac{\partial T}{\partial x}+v\frac{\partial T}{\partial y}+\frac{\partial}{\partial y}(\overline{\tilde{\theta}\tilde{v}})=0 \quad ....(24)$$

The exercise gives us the following result,

$$\frac{\tilde{u}}{u_m}\approx\frac{\tilde{\theta}}{T}\approx\left(\frac{h}{L}\right)^{\frac{1}{2}} \quad ....(25)$$

In order to preserve self-similarity at all heights we must have,

$$\frac{\tilde{u}}{u_m}\approx\frac{\tilde{\theta}}{T}\approx \text{Constant} \quad ....(26)$$

In other words, it can be said that the velocity and temperature fluctuations will have same relative role in their mean profiles. Thus both the mean and fluctuating scales can be represented by a single scale quantity.

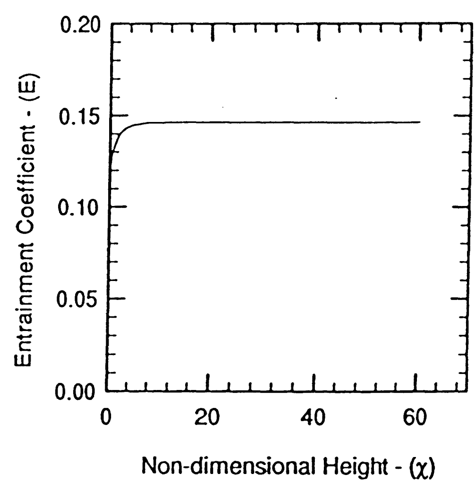

Fig. 11. Change of entrainment coefficient [eq.(22)]

In general, for the velocity distribution across stream wise direction for the wall plume, we may expect that,

$$\frac{u}{u_m}=f(u_m, y, x, h, \text{buoyancy}, \text{viscous}, \text{and frictional forces.}) \quad ......(27)$$

Otherwise,

$$\frac{u}{u_m}=f\left(\frac{y}{h},\frac{x}{h_o},\text{buoyancy}, \text{viscous}, \text{and friction}\right) \quad ....(28)$$

$$\text{Or,} \quad \frac{u}{u_m}=f(\xi,\lambda,\theta) \quad ....(29)$$

where, $\xi = \frac{y}{h}$,

$$\lambda = f_1\left(Re, \frac{h_o}{x}\right), \qquad Re = \frac{Vx}{\nu},$$

$$\theta = f_2\left(S, \frac{h_o}{x}\right), \qquad S = \frac{g(\rho_\infty - \rho)hx}{\nu\rho_\infty V} \quad ...(30)$$

S is the new non-dimensional parameter introduced, which is a relative measure of inertia, buoyancy and viscous forces. S can be viewed as the change of inertia forces as a result of the interactions between the buoyancy and viscous forces. Assuming compete self-similarity in the flow the following equations (31) to (33) alongwith equation (29) can written,

$$-\overline{uv} = u_m^2 g(\xi, \lambda, \theta) \quad ....(31)$$

$$T - T_a = T_m F(\xi, \lambda, \theta) \quad ....(32)$$

and, $$-\overline{\theta v} = T_m u_m H(\xi, \lambda, \theta) \quad ....(33)$$

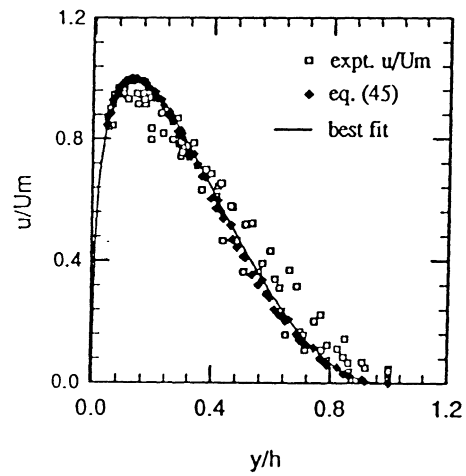

Fig. 12. Velocity distribution in wall plume

Differentiating equation (29), gives,

$$\frac{du}{dx} = f\frac{du_m}{dx} + u_m\Lambda, \quad \text{where}$$

$$\Lambda = -\dot{f}_\xi \frac{\xi}{h}\frac{dh}{dx} + \dot{f}_\lambda \frac{d\lambda}{dx} + \dot{f}_\theta \frac{d\theta}{dx}, \quad \text{and}$$

$$\dot{f}_\xi = \frac{\partial f}{\partial \xi}, \dot{f}_\lambda = \frac{\partial f}{\partial \lambda}, \dot{f}_\theta = \frac{\partial f}{\partial \theta} \quad ....(34)$$

Applying continuity condition in the flow yields,

$$v = -h\int_0^\xi \left(f\frac{du_m}{dx} + u_m\Lambda\right)d\xi. \quad ....(35)$$

The remaining quantities are,

$$\frac{dv}{dy} = -\left(f\frac{du_m}{dx} + u_m\Lambda\right),$$

$$-\frac{\partial}{\partial y}(\overline{uv}) = -u_m^2 \dot{g}_\xi / h \quad ....(36)$$

Substituting these quantities in equations (23), the following equation is obtained,

$$\left(\frac{h}{u_m}\frac{du_m}{dx}\right)f^2 - \left(\frac{dh}{dx}\right)f\dot{f}_\xi\xi + \left(h\frac{d\lambda}{dx}\right)f\dot{f}_\lambda + \left(h\frac{d\theta}{dx}\right)f\dot{f}_\theta$$
$$-\left(\frac{h}{u_m}\frac{du_m}{dx}\right)\dot{f}_\xi\int_0^\xi f d\xi - \left(\frac{dh}{dx}\right)\dot{f}_\xi\int_0^\xi \dot{f}_\xi \xi d\xi$$
$$+\left(h\frac{d\lambda}{dx}\right)\dot{f}_\xi\int_0^\xi \dot{f}_\lambda d\xi + \left(h\frac{d\theta}{dx}\right)\dot{f}_\xi\int_0^\xi \dot{f}_\theta d\xi - \dot{g}_\xi$$
$$= \frac{9.81 h T_m F}{u_m^2 T_a} \quad ....(37).$$

Similar substitutions in energy equation (24) result in

$$\left(\frac{h}{T_m}\frac{dT_m}{dx}\right)fF - \left(\frac{dh}{dx}\right)f\dot{F}_\xi\xi + \left(h\frac{d\lambda}{dx}\right)f\dot{F}_\lambda +$$
$$\left(h\frac{d\theta}{dx}\right)f\dot{F}_\theta - \left(\frac{h}{u_m}\frac{du_m}{dx}\right)\dot{F}_\xi\int_0^\xi f d\xi -$$
$$\left(\frac{dh}{dx}\right)\dot{F}_\xi\int_0^\xi \dot{f}_\xi \xi d\xi + \left(h\frac{d\lambda}{dx}\right)\dot{F}_\xi\int_0^\xi \dot{f}_\lambda d\xi +$$
$$\left(h\frac{d\theta}{dx}\right)\dot{F}_\xi\int_0^\xi \dot{f}_\theta d\xi - \dot{H}_\xi = 0 \quad .....(38)$$

In accordance with similarity assumptions, the coefficients in equations (37) and (38) are constants. Thus finally the following results are obtained,

$$\left.\begin{aligned} &\frac{h}{u_m}\frac{du_m}{dx} = C_1, \quad \frac{h}{T_m}\frac{dT_m}{dx} = C_2, \\ &\frac{dh}{dx} = C_3, \quad \frac{d\lambda}{dx}h = C_4, \quad \frac{d\theta}{dx}h = C_5 \end{aligned}\right\} \quad ..(39)$$

The solutions of the equation (37) and (38) are set below. It can be noted that the average and maximum quantities of various properties are related by a constant factor because of the self similar profiles in velocity and temperature or density defect distributions in the flow.

$$u_m \sim \text{const.} \quad \Rightarrow V \sim \text{const.} \qquad ......(40)$$

$$h \sim x \qquad ....(41)$$

$$T_m \sim \frac{1}{x} \quad \Rightarrow D \sim \frac{1}{x} \qquad ....(42)$$

$$Re \sim x \qquad ....(43)$$

$$S \sim x \qquad ....(44)$$

Comparing equations (40) - (42) and equation (20), it can be inferred that the results from the scaling and similarity analysis do match with the solutions of the physical model of the plume.

5. Velocity Distribution:

Grella and Faeth (1975) measured velocity profiles in a turbulent adiabatic plume at two locations far away from the source. They used the burning of an array of small carbon monoxide jets tangential to the wall as the buoyancy source. Five different source strengths were considered by proper adjustment of the jets.

Table 2: Summary of the plume test conditions

No	V	ho	h	x	D
1	.239	.066	.086	.61	.229
2	.323	.066	.082	.61	.366
3	.238	.066	.146	1.22	.091
4	.337	.066	.177	1.22	.150
5	.483	.066	.150	1.22	.277

Table 3: Values of non-dimensional quantities

No	Re	m	S	n
1	9307	.33	3079	2.4
2	12584	.34	3365	2.44
3	18543	.33	4271	2.25
4	26270	.34	5943	2.38
5	37591	.36	6237	2.4

Further calculations have been performed on their data to extract additional information. The results are shown in Tables 2 and 3. The average quantities are found by integration of the velocity profiles. The summary of the test conditions are shown in Table 2 and various non-dimensional quantities are tabulated in Table 3. In accordance with equation (29) a conjecture, shown in equation (45), is proposed. It has been tested in all five conditions of the plume and found to be correlating satisfactorily. The values of the exponents in the conjecture are shown in Table 3. The basic form of proposed profile is obtained from the two boundary conditions at $x = 0$ and ∞ for velocity. However, the conjecture is,

$$\frac{u}{u_m} = C\xi^{C_x \ln[\frac{h_o}{x} Re]} (1-\xi)^{C_y \ln[\frac{h_o}{x} S]} \qquad ......(45)$$

where,

$$\xi = \frac{y}{h}, \quad m = C_x \ln[\frac{h_o}{x} Re], \quad n = C_y \ln[\frac{h_o}{x} S] \qquad .....(46)$$

Constant C can be found from the condition of the maximum velocity. Constants C_x and C_y, with numerical values of 1/21 and 45/109 respectively, have been determined from the experimental results. Figure 12 shows the experimental data, velocities evaluated using equation (45) and the best fit curve through the evaluated values. The values of the exponents m and n are shown in Table 3 for five cases. These values vary in the order of 7-8% which indicates reasonable degree of consistency in the conjecture.

6. CONCLUSION:

An analytical model, based on integral methods, to predict spatially averaged streamwise flow properties is presented here. Using this model numerical simulations were carried out. An analysis has been made in the flow domain to characterise the flow variables with the assumption of self-similarity in the flow. Numerical results have been found to match well with the analysis. Also a conjecture has been proposed for the velocity distributions in the flow. It has been tested with experimental results and found to be correlating satisfactorily.

Nomenclature :

C_1, C_2, C_3, C_4, C_5	constants
C_x, C_y	constants
C_f	friction factor
C_p	heat capacity (KJ/kgK)
D, D_o	density defect (m/s^2)
E	entrainment coefficient
Fr, Fr_o	Froud number
g	acceln. due to gravity (m/s^2)
h, h_o	plume width (m)
q''	heat loss (W/m^2)
Re	Reynolds number
T	temperature (K)
u_x, V, V_o	velocity (m/s)
u_m	maximum velocity (m/s)
x, y	coordinate axes
ρ	density (kg/m^3)
χ, ξ	non-dimensional coordinate
η	non-dimensional width
α	constant, Eq. (22)
λ, θ	functions, Eq. (30)
Λ	function, Eq. (34)

subscripts

∞, a	ambient conditions
o	initial conditions
m	maximum conditions
ent	entrainment

REFERENCES:

Alpert, R. L., "Turbulent Ceiling-Jet Induced by Large Scale Fires", *Combust. Sci. and Technology*, 11, (197-213)1975.

Beyler, C. L., "Fire Plumes and Ceiling Jets", *Fire Safety J.*, 11, (53-75)1986.

Gebhart, B., Jaluria, Y., Mahajan, R. L., and Sammkia, B., *Buoyancy Induced Flows and Transport*, 1st. ed., Hemisphere Publishing corp., New York, USA.

Grella, J. J., and Faeth, G. M., "Measurements in a Two Dimensional Thermal Plume Along a Vertical Adiabatic Wall", *J. Fluid Mech.*, 71, part 4, (701-710)1975.

Hasemi, Y., and Tokunaga, T., *ASME J. Heat Tr.*, 108, 882(1986).

Lee, S. L., and Emmons, H. W., "A Study of Natural Convection Above a Line Fire", *J. Fluid Mech.*, 11, (353-368)1961.

List, E. J., "Turbulent Jets and Plumes", *Ann. Rev. Fluid Mech.*, 14, (189-212)1982.

Morton, B. R., Sir Taylor, G., and Turner, J. S., "Turbulent Gravitational convection from Maintained and Instantaneous Sources", *Proc. Royal Soc. A.*, 234, (1-23)1956.

Rouse, H., Yih, C. S., and Humphreys, H. W., "Gravitational Convection from a Boundary Source", *Tellus*, 4, (201-210)1952.

Sparrow, E. M., Patanker, S. V., Abdel-Wahed, R. M., "Development of Wall and Free Plume Above a Heated Vertical Plate", *J. Heat Tr.*, 100, (184-190)1978.

Tennekes, H., and Lumley, J. L., *A First Course in Turbulence*, The MIT Press, Cambridge, London, UK.